VNU Journal of Science: Mathematics - Physics

Journal homepage: https://js.vnu.edu.vn/MaP

Original Article

HRBE Diagrams and Thermoluminescence of B_2O_3-TeO_2-Li_2O-CaO Glass Doped with Lanthanide Ions

Phan Van Do[1,*], Vu Phi Tuyen[2], Nguyen Xuan Ca[3]

[1]*Thuyloi University, 175 Tay Son, Hanoi, Vietnam*

[2]*National Institute of Information and Communications Strategy - MIC, 115 Tran Duy Hung, Hanoi, Vietnam*

[3]*Institute of Science and Technology, TNU-University of Sciences, Thai Nguyen, Vietnam*

Received 8th October 2025
Revised 29th November 2025; Accepted 6th April 2026

Abstract. In this study, undoped and Ln^{3+}-doped $40B_2O_3$-$30TeO_2$-$15Li_2O$-15CaO (BTLC) glasses were fabricated using the melt-quenching method. Using Dorenbos's models, we constructed diagrams of the ground energy levels for the 4f states of divalent and trivalent lanthanide ions within the bandgap of the glass, based on the photoluminescence excitation spectra of Eu^{3+} and Ce^{3+} ions. Predictions for the selection of Ln^{3+} impurities in the thermoluminescent (TL) material were made based on the analysis of these diagrams, with Ce^{3+} and Tb^{3+} ions predicted to act as recombination centers. The validity of these predictions was checked by measurements of the TL glow curves and TL spectra for BTLC:Ce^{3+} and BTLC:Tb^{3+} samples.

Keywords: Dorenbos's model, Thermoluminescence material.

1. Introduction

Oxide glasses doped with trivalent lanthanide ions (Ln^{3+}) have long attracted attention as research subjects for spectroscopic applications, including lasers, dosimetry, and lighting. The advantages of these materials include ease of fabrication, high mechanical and chemical durability, and high solubility of rare-earth ions [1-3]. One of the most interesting glass matrices is the borate host, as it exhibits unique spectral properties, including strong emission, a large emission cross-section, and high quantum efficiency [1, 2]. In the field of radiation safety, borate glass doped with Ln^{3+} ions is a promising

* Corresponding author.
E-mail address: phanvando@tlu.edu.vn

https//doi.org/10.25073/2588-1124/vnumap.4170

candidate for dosimeters in nuclear medicine, owing to its effective atomic number being nearly equivalent to that of biological tissue [4-8]. Recently, numerous fundamental studies have investigated the thermoluminescent (TL) properties of these compounds, including $LiCaBO_3:Ce^{3+}$, Sm^{3+} [4], $Li_2B_4O_7:Dy^{3+}$, Ce^{3+} [5], $NaBaBO_3:Tb^{3+}$ [7], and $LiCaF_2BTeO_4:Ce^{3+}$, Tb^{3+} [8] glasses. The obtained demonstrate the advantages of this material, including high dose sensitivity and low signal attenuation. In addition, studies have shown that Ln^{3+} ions may act as luminescence or recombination centers in the TL process [6-8]. Nonetheless, it is important to note that the TL materials currently in use were discovered serendipitously. In the past, it was widely believed that the TL properties of materials could not be predicted or modeled theoretically in advance. Therefore, the prediction of thermoluminescent materials, including both their matrix and dopant ions, is a highly significant area of research. In 2003 and 2013, Dorenbos published two models-the charge transfer [9, 10] and chemical shift [11, 12] models-for constructing the ground-state energy diagrams of Ln^{2+} and Ln^{3+} ions relative to the host (host-referred binding energy, HRBE) or the vacuum (vacuum-referred binding energy, VRBE). The main advantage of these diagrams is their strong predictive capability regarding the fluorescence and thermoluminescence properties of Ln ions, as well as in guiding the design of functional materials doped with Ln ions [9-12].

In this work, we construct the HRBE diagram for Ln ions in BTLC glass with a composition of $40B_2O_3$-$30TeO_2$-$15Li_2O$-15CaO. The selection of rare-earth ions for doping in thermoluminescent materials was guided by these diagrams. To validate these predictions, several studies on the thermoluminescence of BTLC:Ln^{3+} glasses were also performed.

2. Experiments

BTLC glasses undoped and doped with Ln^{3+} (Ln = Eu, Ce, and Tb) ions were fabricated using the melt quenching method from the initial chemicals of Li_2O, H_3BO_3, TeO_2, and Ln_2O_3 (Ln = Ce, Tb, and Eu). Details of material fabrication steps have been presented in our recent publication [3-5]. The photoluminescence (PL), photoluminescence excitation (PLE), and thermoluminescence spectra were recorded by a Fluorolog-3 spectrometer, model FL3-22, Horiba Jobin Yvon. The TL glow curves of materials were measured using a Hashaws TLD-5500 reader (USA). The TL measurements were carried out in the temperature region of 50-400 ºC with a heating rate β of 5 ºC/s. Irradiation of the beta-ray to the samples was performed with a ^{90}Sr source.

3. Results and Discussion

3.1. Constructing the HRBE Diagrams of the Ln^{2+} and Ln^{3+} Ions in the Bandgap of the Glass

The spectroscopic properties of Ln-ion-activated inorganic compounds depend not only on the energies of the excited 4f and 5d states, but also on their positions relative to the energy bands of the host materials [9-12]. Thus, constructing the ground-state energy (GE) level diagram of Ln ions is of high practical significance. In principle, the ground-state energy (GE) positions of Ln ions can be determined experimentally. Specifically, the ground energy levels of the 4f states for Ln^{2+} and Ln^{3+} in a host are equal to the charge transfer (CT) energies of the corresponding Ln^{3+} and Ln^{4+} ions in that host. However, such measurements are highly complex and costly, as these energies typically lie in the deep ultraviolet region [9, 10]. To date, we have observed the CT bands of only a few Ln^{3+} ions, such as Eu^{3+} and Sm^{3+}, whereas the CT bands of Ln^{4+} ions have not yet been recorded. However, according to the Dorenbos models [9-12], the GE levels of all Ln^{2+} and Ln^{3+} ions in the material can be determined solely from the PLE spectra of Eu^{3+} and Ce^{3+} ions.

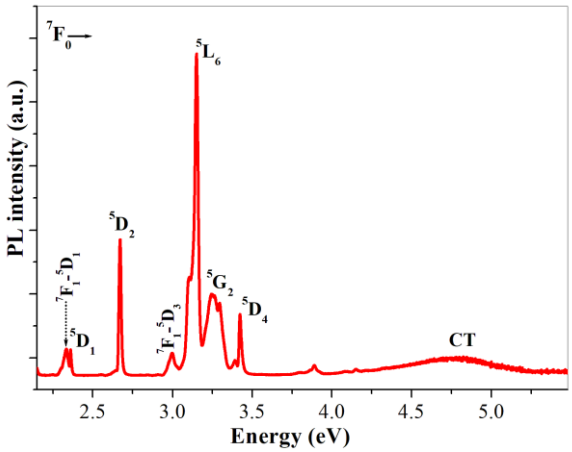

Figure 1. PLE spectrum of the Eu^{3+} ion in BTLC:Eu^{3+} glass.

Fig. 1 presents the PLE spectrum of the Eu^{3+} ion in BTLC:Eu^{3+} glass, monitored at the emission wavelength of 612 nm. This spectrum comprises the characteristic transitions of the Eu^{3+} ion from the ground levels $^7F_0$ or $^7F_1$ to the excited levels of the $4f^6 5d^0$ configuration [13], as attributed in Fig. 1. In addition, the PLE spectrum exhibits a broad band centered at 4.76 eV, attributed to the charge transfer of the Eu^{3+} ion in this host [3]. This value represents the energy difference between the ground state of Eu^{2+} and the top of the valence band in the material [9, 10], denoted as $E_{4f}(Eu^{2+}, BTLC)$. For other Ln^{3+} ions, their charge transfer bands cannot be recorded. However, the difference between the E_{4f} energy of Eu^{2+} and that of any Ln^{2+} ion ($\Delta E_{4f}(Eu^{2+}, Ln^{2+})$) depends solely on the type of Ln ion and is independent of the host, as reported by Dorenbos [9]. Thus, the ground energy location of any Ln^{2+} ion is calculated by the following formula [9, 10]:

$$E_{4f}(Ln^{2+}, BTLC) = E_{4f}(Eu^{2+}, BTLC) + \Delta E_{4f}(Eu^{2+}, Ln^{2+}) \quad (1)$$

The value of the $E_{4f}(Ln^{2+}, BTLC)$ of all Ln^{2+} in the bandgap for the BTLC glass is shown in column 2 of Table 1. The plot of the ground energy level of the $4f^n$ state on the number of electrons in the $4f^n$ state for all Ln^{3+} ions is indicated by the zig-zag a in Fig. 2.

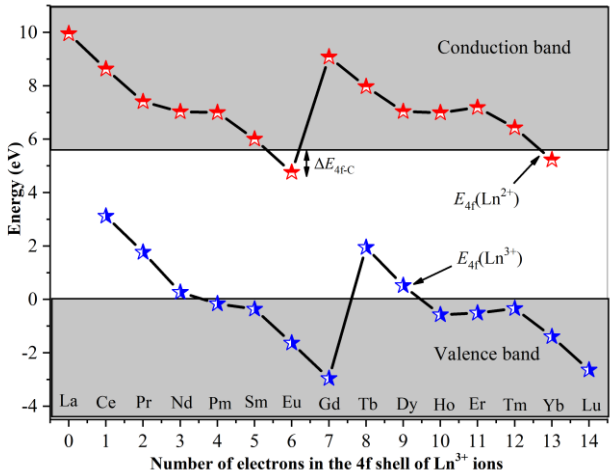

Figure 2. HRBE diagrams of the 4f state for Ln^{2+} and Ln^{3+} ions in BTLC glass.

To determine the GE levels of the 4f states for Ln^{3+} ions, $E_{4f}(Ln^{3+}, BTLC)$, we apply the chemical shift model. According to this model, the $E_{4f}(Eu^{3+}, BTLC)$ value for the Eu^{3+} ion is calculated using the following relationship [11, 12]:

$$E_{4f}(Ln^{3+}, BTLC) = E_{4f}(Eu^{2+}, BTLC) - U(Eu^{2+}, BTLC) \quad (2)$$

Here, the quantity $U(Eu^{2+}, BTLC)$, referred to as the "Coulomb repulsion energy", is calculated using the following expression [11]:

$$U\left(Eu^{2+}, BTLC\right) = 5.44 + 2.834 \exp\left\{-\frac{\varepsilon_c(BTLC)}{2.2}\right\} \quad (3)$$

here, $\varepsilon_C(BTLC)$, in units of eV, is the centroid shift of the 5d state of the Ce^{3+} ion in the material. It is related to the energies of the transitions from the $^2F_{5/2}$ ground level of the $4f^1 5d^0$ configuration to the $5d_i$ (i = 1-5) levels of the $4f^0 5d^1$ configuration in Ce^{3+}, as given by the formula [11]:

$$\varepsilon_c = 6.35 - \frac{1}{5}\sum_{i=1}^{5} E_{fdi}\left(Ce^{3+}, BTLC\right) \quad (4)$$

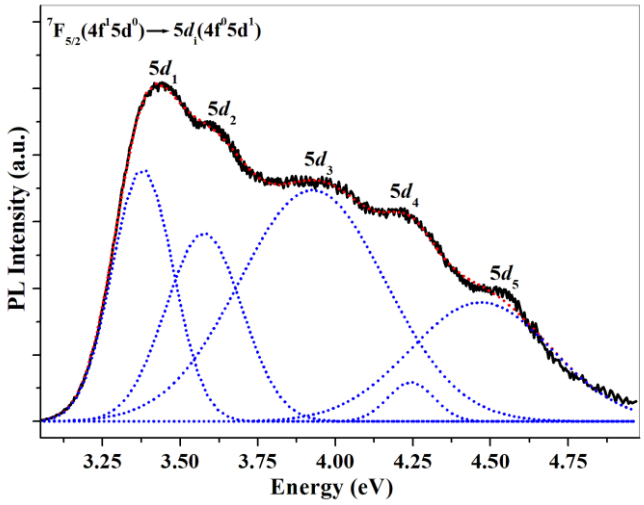

Figure 3. PLE spectrum of the Ce^{3+} ion in BTLC:Ce^{3+} glass.

Fig. 3 shows the PLE spectrum of Ce^{3+} ions in BTLC glass, observed at an emission wavelength of 415 nm. The spectrum indicates a broad band resulting from the superposition of five transitions from the $^2F_{5/2}$ ground state to the $5d_i$ (i = 1-5) excited levels [3]. The peak positions of these bands are located at 3.40, 3.62, 3.95, 4.24, and 4.51 eV, respectively. Using these transition energies and Eqs. (3) and (4), the values of the $\varepsilon_C(BTLC)$ and $U(Eu^{2+}, BTLC)$ were determined to be 2.41 and 6.39 eV, respectively. Consequently, the ground-state energy of the 4f level of the Eu^{3+} ion was determined to be $E_{4f}(Ln^{3+}, BTLC)$ = -1.63 eV. Based on the energy differences between the 4f ground state of Eu^{3+} and those of other Ln^{3+} ions reported in Ref. [11], the values of $E_{4f}(Ln^{3+}, BTLC)$ for the remaining Ln^{3+} ions were determined and are listed in Column 4 of Table 1. The dependence of the 4f ground-state energy of Ln^{3+} ions on the number of 4f electrons is indicated by the zigzag b in Fig. 2.

To find the energy separation between the ground state of the Ln^{2+}:4f level and the bottom of the conduction band ($\Delta E_{4f\text{-}C}$), the bandgap energy E_g of the material must first be determined. Accordingly, $\Delta E_{4f\text{-}C}$ value is given by $\Delta E_{4f\text{-}C} = E_g - E_{4f}(Ln^{2+})$. For the BTLC glass, the bandgap energy E_g was obtained from the optical absorption spectrum using the Tau'c method, which was described in detail in our recent

studies [3, 8]. Fig. 4 shows the optical absorption spectrum of undoped BTLC glass, with the inset presenting the plot of $(\alpha.hv)^{1/2}$ versus photon energy hv. From this plot, the bandgap energy E_g was determined to be 5.75 eV, and the energy separation $\Delta E_{4f\text{-}C}$ for all Ln^{2+} ions in BTLC glass was calculated and listed in Column 5 of Table 1.

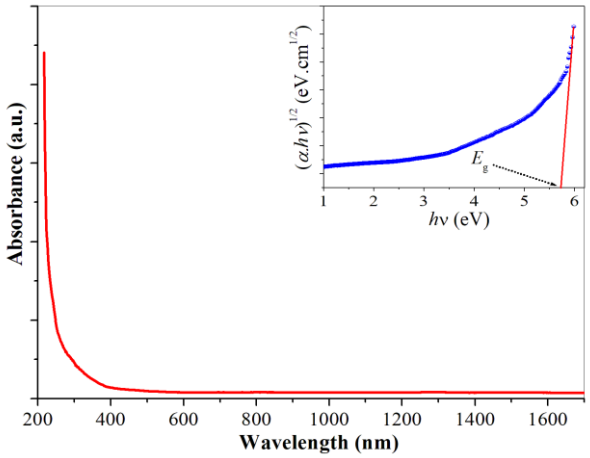

Figure 4. Absorption spectrum of the BTLC host. Inset: the plot of $(\alpha.hv)^{1/2}$ vs hv.

Table 1. The location of the ground energy levels of the $4f^n$ (n = 0-14) state for divalent and trivalent lanthanide ions in the BTLC glass. All parameters in eV units

Lanthanide	n	$E_{4f}(Ln^{2+}$, BTLC)	$E_{4f}(Ln^{3+}$, BTLC)	$\Delta E_{4f\text{-}C}$ (Ln^{2+})
La	0	9.95	-	-4.20
Ce	1	8.63	3.61	-2.88
Pr	2	7.41	1.77	-1.66
Nd	3	7.03	0.27	-1.28
Pm	4	7.00	-0.16	-1.25
Sm	5	6.01	-0.36	-0.26
Eu	6	4.76	-1.63	0.99
Gd	7	9.08	-2.96	-3.33
Tb	8	7.97	1.95	-2.22
Dy	9	7.04	0.52	-1.29
Ho	10	6.99	-0.57	-1.24
Er	11	7.19	-0.51	-1.44
Tm	12	6.43	-0.34	-0.68
Yb	13	5.23	-1.39	0.52
Lu	14	-	-2.64	-

One of the applications of the HRBE diagram is its ability to predict suitable rare-earth ions for thermoluminescent materials. If an Ln^{2+} ion has a 4f ground state located a few eV below the bottom of the conduction band, the corresponding Ln^{3+} ion may act as an electron trap. Conversely, if an Ln^{3+} ion possesses a 4f ground state situated a few eV above the top of the valence band, it may serve as a hole-trap center [9, 14, 15]. During irradiation of the material with ionizing radiation, electrons and holes are generated. Electrons may be captured by Ln^{3+} traps, forming Ln^{2+} via $Ln^{3+} + e^- \rightarrow Ln^{2+}$, while holes may be trapped at centers according to $Ln^{3+} + h^+ \rightarrow Ln^{4+}$. Upon heating to sufficiently high temperatures,

electrons are released from the Ln^{2+} traps and recombine with holes at the Ln^{4+} centers through $Ln^{2+} – e^- \rightarrow (Ln^{3+})^*$, and $Ln^{4+} + e^- \rightarrow (Ln^{3+})^*$. These processes generate Ln^{3+} ions in excited states ($(Ln^{3+})^*$), which finally relax to their ground state by emitting characteristic luminescence.

As shown in Fig. 2 and Table 1, the 4f ground-state levels of Eu^{2+} and Yb^{2+} ions are located 0.99 and 0.52 eV below the bottom of the conduction band, respectively. Therefore, the Eu^{3+} and Yb^{3+} ions can act as electron traps in the TL process, with activation energies of approximately 0.99 and 0.52 eV, respectively [14, 15]. For other Ln^{2+} ions, the 4f ground-state level lies within the conduction band. Consequently, the corresponding Ln^{3+} ions cannot be considered effective electron traps in the TL process of BTLC glasses [14]. Nevertheless, thermoluminescence signals can still be observed for these ions. This behavior is attributed to energy transfer from intrinsic recombination centers to the Ln^{3+} ions [4, 5]. Fig. 2 also shows that the 4f ground-state levels of the Ce^{3+}, Pr^{3+}, and Tb^{3+} ions are located several eV above the top of the valence band; therefore, these ions can act as hole-trap centers in the TL process. To verify the reliability of these predictions, the TL properties of BTLC glasses singly doped with Ce^{3+} or Tb^{3+} ions would be investigated.

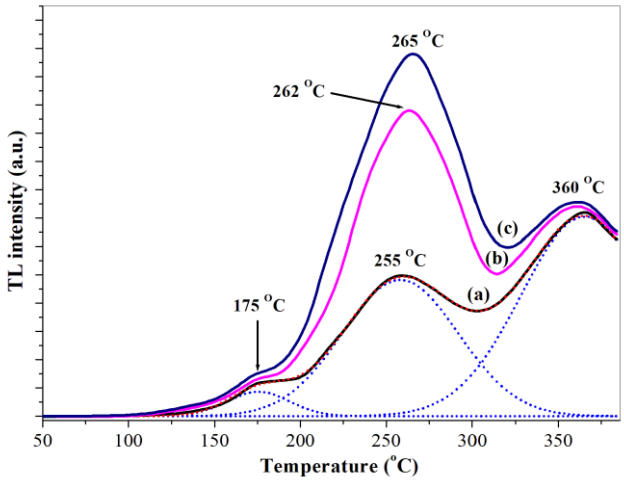

Figure 5. TL glow curves of the glass samples: a) undoped BTLC, b) BTLC:Tb^{3+}, and BTLC:Ce^{3+}.

Fig. 5 shows the TL glow curves of the undoped BTLC (curve a), BTLC:Tb^{3+} (curve b), and BTLC:Ce^{3+} (curve c) samples. Before TL measurements, the samples were irradiated with beta rays at a dose of 10 Gy. For undoped BTLC, the TL glow curve exhibits two distinct peaks at 255 °C and 367 °C, along with a shoulder around 175 °C. The TL process can be explained as follows: In this case, defects generated during the fabrication process or induced by irradiation may serve as hole or electron traps (collectively referred to as intrinsic centers or traps). The electrons can be captured by the centers above the Fermi level (electron traps), while the holes are trapped by the centers below the Fermi level (recombination centers); When the material is heated, the electrons are released from the traps and move to recombine with the holes at the hole centers; The energy released from this recombination can be emitted as TL light [4, 5, 16]. Using the method of peak shape [4], the active energy (E_T) and escape frequency (s) were calculated for all bands to be (0.62 eV, $1.46.10^7$ s^{-1}), (0.94 eV, $1.92.10^8$ s^{-1}), and (1.36 eV, $3.15.10^8$ s^{-1}) for the 178, 260, and 367 °C, respectively.

When Ce^{3+} or Tb^{3+} ions are doped into the glass, the TL curve also exhibits three bands, similar to that of the undoped sample. However, the second band is slightly shifted toward higher temperatures (262 and 265 °C for BTLC:Tb^{3+}, and BTLC:Ce^{3+}, respectively), and the TL intensity increases

significantly, while the other bands remain almost unchanged. The TL intensities of the BTLC:Tb^{3+}, and BTLC:Ce^{3+} samples are enhanced by factors of 2.52 and 2.63, respectively, relative to the undoped BTLC. The results obtained suggest that the trap locations and the characteristics of the recombination centers corresponding to peaks 1 and 3 are inherently determined by the host matrix, rather than being affected by impurities. These traps and centers are typically intrinsic defects or non-bridging oxygen centers that are inherently present in the glass matrix [4-8]. The enhancement of the TL intensity in the second band may result from the incorporation of Ce^{3+} or Tb^{3+} ions into the glass matrix.

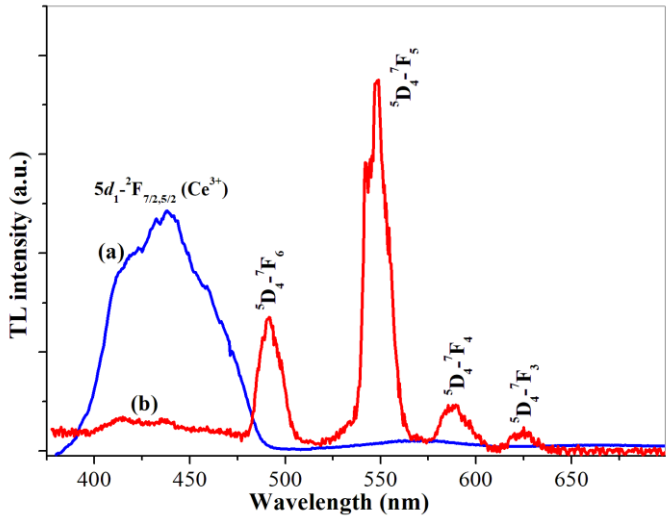

Figure 6. TL spectra of the first band for: a) BTLC:Ce^{3+} glass, and b) BTLC:Tb^{3+} glass.

To investigate the nature of the recombination centers corresponding to the second band, TL spectra were recorded at approximately 262 and 265 °C for the BTLC:Tb^{3+}, and BTLC:Ce^{3+} samples, respectively. Before these measurements, the samples were exposed to the beta rays with a dose of 10 Gy. The results are shown in Fig. 6. It can be observed that the TL spectra at the second peak exhibit the characteristic emission bands of Ce^{3+} and Tb^{3+} in the BTLC:Ce^{3+} and BTLC:Tb^{3+} samples, respectively. Based on these measurements and previously published studies, we propose two possible origins for the emission bands of the second peak as follows:

i) *The Ce^{3+} and Tb^{3+} ions are the hole and luminescence centers*. The HRBE diagrams (Fig. 2) and Table 1 indicate that the location of the 4f ground energy level of the Ce^{3+} and Tb^{3+} is 3.61 and 1.95 eV higher than the top of the valence band, respectively. Thus, they may have the potential to capture holes generated during irradiation and become Ce^{4+} and Tb^{4+} centers, whereas the electrons may be captured at the traps. Heating the material releases electrons in the traps, which then move to recombine with holes at these centers: $Ce^{4+} + e^- \rightarrow Ce^{3+}$, and $Tb^{4+} + e^- \rightarrow Tb^{3+}$. The Ce^{3+} and Tb^{3+} ions are in the excited state, then they relax to their ground state by emitting the characteristic luminescence [14, 15]. The selective enhancement of the second TL band (~262–265 °C) upon doping with Ce^{3+} or Tb^{3+} ions is due to the formation of new traps and radiative recombination centers that match the energy of this band. These ions mainly interact with electrons from the second TL band traps, enhancing radiative recombination and TL intensity, while the other bands remain largely unaffected due to energetic mismatch or weak interaction with the dopants.

ii) *The Ce^{3+} and Tb^{3+} ions are the luminescent centers through the energy transfer.* With this assumption, the TL process of the second band appears similar to that of the first and third bands, i.e.,

related to the defects of the host matrix. However, the Ln^{3+} ions may be located near the recombination centers corresponding to the second band, so the energy released during recombination is transferred to the Ln^{3+} ions. These ions are then transferred to the excited state and finally relax to the ground state through light emission [4-8]. This process allows the observation of TL signals from Ln^{3+} ions, even when the corresponding Ln^{2+} ions lie within the conduction band of the material.

In this work, a commercial TLD Reader (Harshaw 3500) equipped with a PMT (model R6231) was used to measure the TL glow of the samples. This system exhibits high sensitivity in the visible and near-UV region from 300 to 600 nm, with peak quantum efficiency between 400 and 450 nm. For the undoped BTLC glass, the intrinsic defects act as the electron traps. The emission region of these centers is usually in the UV (300-400 nm) [8], which is not sensitive to the PMT. For the Ce^{3+} and Tb^{3+} ions, their emission is in the sensitive region of the PMT. When doped into the glass matrix, Tb^{3+} or Ce^{3+} may act as recombination centers or luminescent centers. The probability of radiative recombination at Ln centers may be higher than that at intrinsic recombination centers. The efficient energy transfer from the intrinsic recombination centers to the Tb^{3+} or Ce^{3+} generates the emission band in the sensitive region of the PMT. In addition, an increase in the concentration of the Ln^{3+} impurities also leads to an increase in the number of defects. All of these factors contribute to an enhancement of the TL intensity.

4. Conclusion

Using the melt quenching method, the BTLC glasses, undoped and doped with Eu^{3+}, Tb^{3+}, and Ce^{3+} ions, were successfully fabricated. Using Tau's method, the bandgap of the material was determined to be 5.75 eV. The schemes of the 4f ground energy levels of the Ln^{3+} and Ln^{2+} ions in glass have been constructed. Based on these diagrams, some Ln^{3+} ions were predicted to play the role of electron traps (Eu^{3+}, Yb^{3+}) or hole centers (Ce^{3+}, Tb^{3+}) in the thermoluminescence process. These predictions were checked via measurements of the TL glow curve and TL spectra of the BTLC:Ce^{3+} and BTLC:Tb^{3+} samples. The TL glow curve of the BTLC host includes two bands centered at 175, 255 and 360 ^{o}C. The electron traps and recombination centers in this TL process are related to the defects in the host matrix. For the BTLC:Ce^{3+} and BTLC:Tb^{3+} glasses, the second TL band is related to the presence of the Ln^{3+} doped into the material. Doping of Tb^{3+} and Ce^{3+} ions into the BTLC glass increased the thermoluminescence intensity of the second band by 2.53 and 2.52 times compared to the undoped sample.

Acknowledgments

This research is funded by Vietnam National Foundation for Science and Technology Development (NAFOSTED) under grant number 103.03–2021.75.

References

[1] R. N. Sheetal, V. Kumar, S. Dahiya, N. Deopa, R. Punia, A. S. Rao, Judd-Ofelt Itemization and Influence of Energy Transfer on Sm^{3+} ions Activated B_2O_3–ZnF_2–SrO–SiO_2 Glasses for Orange-red Emitting Devices, J. Lumin, Vol. 229, 2021, Article numberr. 117651, https://doi.org/10.1016/j.jlumin.2020.117651.

[2] A. M. Babeer, H. Y. Amin, M. I. Sayyed, A. E. Mahmoud, M. S. Sadeq, Effect of Mixed Rare Earth Cations on Structure, Optical, Mechanical, and Radiation Shielding Parameters of Na_2O-B_2O_3 Glass, Radiat. Phys. Chem, Vol. 220, 2024, Article number. 111661, https://doi.org/10.1016/j.radphyschem.2024.111661.

[3] P. V. Do, T. Ngoc, N. T. Hien, L. D. Thanh, N. M. Hung, T. T. C. Thuy, P. T. Du, N. T. Huong, HRBE Diagrams for Lanthanides and the Temperature Dependence of Tb^{3+} Luminescence in Zinc-Sodium-Lanthanum-Borate Glass, Physica B. Vol. 641, 2022, Article number. 414089, https://doi.org/10.1016/j.physb.2022.414089.

[4] T. Ngoc, N. X. Ca, N. V. Ha, L. D. Thanh, D. N. Binh, T. T. C. Thuy, N. V. Nghia, V. X. Phuc, P. V. Do, Studying the Structure, Photoluminescence and Thermoluminescence Properties of LiCaBO3 Pseudoternary Glass-Ceramic Co-doped with Ce^{3+}, Sm^{3+} ions, Opt Mater. Vol. 157, 2024, Article number. 116100, https://doi.org/10.1016/j.optmat.2024.116100.

[5] T. Ngoc, N. X. Ca, N. V. Ha, T. T. C. Thuy, N. T. Huong, L. D. Thanh, N. V. Nghia, P. V. Do, Thermoluminescence Properties of the $Li_2B_4O_7:Dy^{3+},Ce^{3+}$ Glasses and Their Application Potential in the Dosimetry Field, Opt Mater. Vol. 158, 2025, Article number. 116443, https://doi.org/10.1016/j.optmat.2024.116443.

[6] M. Sonsuz, M. Topaksu, J. Hakami, N. Can, Synthesis and Thermoluminescence Study of Eu-doped Novel $LaBO_3$ Phosphor: Heating Rate, Dose Response, Trapping Parameters, Radiat. Phys. Chem, Vol. 201, 2022, Article number. 110412, https://doi.org/10.1016/j.radphyschem.2022.110412.

[7] M. Oglakci, M. Topaksu, Y. Alajlani, N. Can, E.E. Karali, Thermal Quenching and Evaluation of Trapping Parameters of Thermoluminescence Glow-Peaks of Beta Irradiated $NaBaBO_3:Tb^{3+}$ for TLD Applications, J. Lumin. Vol. 244, 2022, Article number. 118731, https://doi.org/10.1016/j.jlumin.2022.118731.

[8] T. Ngoc, N. X. Ca, N. V. Ha, T. T. C. Thuy, L. D. Thanh, N. D. A. Tuan, P. V. Do, Structure, Optical, and Thermoluminescence Properties of $LiCaF_2BTeO_4$ Glass-Ceramic Co-doped with Ce^{3+} and Tb^{3+} ions, Ceram. Int. Vol. 51, No. 25, 2025, pp. 44126-44136, https://doi.org/10.1016/j.ceramint.2025.07.144.

[9] P. Dorenbos, Locating Lanthanide Impurity Levels in the Forbidden Band of Host Crystals, J. Lumin. Vol. 108, No. 1-4, 2004, pp. 301-305, https://doi.org/10.1016/j.jlumin.2004.01.064.

[10] P. Dorenbos, Systematic Behaviour in Trivalent Lanthanide Charge Transfer Energies, J. Phys. Condens. Matter Vol. 15, No. 48, 2003, pp 8417–8434, doi:10.1088/0953-8984/15/49/018.

[11] P. Dorenbos, Modeling the Chemical Shift of Lanthanide 4f Electron Binding Energies, Phys. Rev. B. Vol. 85, 2012, Article number. 165107, https://doi.org/10.1103/PhysRevB.85.165107.

[12] P. Dorenbos, Ce^{3+}:5d-Centroid Shift and Vacuum-Referred 4f-Electron Binding Energies of all Lanthanide Impurities in 150 Different Compounds, J. Lumin. Vol. 135, 2013, pp 93-104, https://doi.org/10.1016/j.jlumin.2012.09.034.

[13] W.T. Carnall, P.R. Flields, K. Rajnak, Electronic Energy Levels of Trivalent Lanthanide Aquo Ions. IV. Eu^{3+}, J. Chem. Phys. Vol. 49, No. 10, 1968, pp. 4450-4455, https://doi.org/10.1063/1.1669896.

[14] P. Dorenbos, A. J J. Bos, Lanthanide Level Location and Related Thermoluminescence Phenomena, Radiat. Meas., Vol. 43, No. 2-6, 2008, pp. 139-145, https://doi.org/10.1016/j.radmeas.2007.10.007.

[15] A. H. Krumpel, E. V. D. Kolk, D. Zeelenberg, A. J. J. Bos, K. W.Kramer, P. Dorenbos, Lanthanide 4f-Level Location in Lanthanide Doped and Cerium-Lanthanide Co-doped $NaLaF_4$ by Photo-and Thermoluminescence, J. Appl. Phys., Vol. 104, 2008, Article number. 073505, https://doi.org/10.1063/1.2955776.

[16] V. X. Quang, N. M. Khaidukov, V. N. Makhov, N. T. Thanh, N. X. Ca, L. D. Thanh, H. V. Tuyen, T. Ngoc, P. V. Do, Studying the Photo-, Thermo-luminescence Properties and Energy Transfer Processes in $K_2Y_{1-x}Eu_xF_5$ Single Crystals, J. Lumin. Vol. 286, 2025, Article number. 121405, https://doi.org/10.1016/j.jlumin.2025.121405.